SERS and Raman imaging as a new tool to monitor dyeing on textile fibres

Sara Fateixa, Manon Wilhelm, Helena I. S. Nogueira, Tito Trindade*

Department of Chemistry- CICECO
University of Aveiro
3810-193 Aveiro
Portugal

*Corresponding author

Phone: +351 234 370 726
FAX: +351 234 370 084
E-mail:

Abstract

Textile fibres containing Ag nanoparticles have been widely explored for a number of antimicrobial fabrics. Moreover, it is well known that textile dyeing is a critical stage in the manufacture thereof. This research shows that SERS and Raman imaging can be used with advantage in the monitoring of this process. Using Ag containing linen fibres stained with methylene blue (MB) it was possible to map the local distribution of the MB dye in the fibres by Raman imaging. MB was selected as the SERS molecular probe and as a model dye. Composites of linen fibres and Ag nanoparticles were prepared by distinct methods and used as SERS substrates in order to evaluate the effect of the preparative method on the Raman images. Our results demonstrate that by using Raman imaging associated to the presence of Ag nanoparticles it is possible to distinguish the local distribution of the dye on the textile surface. This investigation allows to foreseeing the use of this technique in terms of quality control of Ag containing fabrics, which is a market in great expansion.

Keyword: textile nanocomposites, Raman imaging, silver nanoparticles, SERS, methylene blue

Introduction

In the past decade, the textile industry has applied new techniques for the deposition of nanosized particles on textile fibres in order to enhance properties of conventional fabrics.[1-7] Moreover, the new functionalities arising from the incorporation of metal nanoparticles (NPs) on textile fibres make them good candidates in domains such as wound dressing, smart textiles, water treatment, biosensors and paper industry.[8-10] In this context, silver NPs have been used due to their antimicrobial,[5,10-12] catalytic[13] or conducting[12] properties. For example, bandages and clothes silver-enabled for antibacterial and antifungal purposes became wide spread on the market.[14] Several methods have been reported in the literature for the incorporation of such nanophases in textiles.[5,10-16] For instance, Ag NPs can be obtained directly on the surface of fibres by sputtering and by diverse chemical methods.[5,15] An example of the latter involves the treatment of the fibres with aqueous $AgNO_3$, which then act as platforms for heterogeneous nucleation of the Ag NPs under reductive conditions.[15] Alternatively ex situ methods can be employed, in which previously prepared Ag NPs are attached a posteriori on the substrate by blending16 or by electrostatic assembly such as layer-by-layer (LBL) method.[10,17] The LBL method involves the alternative deposition of positive and negative polyelectrolytes on a substrate such as fibres, together with the adsorption of colloidal metal NPs.[10,11,18] In both cases, surface chemical modification strategies can be used in order to promote the adhesion of the Ag NPs onto the fibres.

The materials composed by textile fibres and metal NPs are normally characterized by instrumental techniques such as UV-Visible absorption spectroscopy, scanning electron microscopy (SEM) and atomic force microscopy (AFM). These techniques not only allow to confirm the presence of the metal on the fibres but also help to study the morphology and the homogeneity of the composites.[5,18] In this work, we demonstrate that Raman imaging techniques coupled to Surface Enhanced Raman Scattering (SERS) methods can be a valuable asset to complement such characterization, namely in aspects crucial to the performance of functional fabrics. Indeed, it is now well established that Ag NPs can be used as platforms that strongly enhance the Raman signal of molecules that interact with their metal surfaces.[19-25]

Hence, there has been an huge increase on the number of SERS studies using Ag NPs, as well as with other types of metal nanostructures, that show the wide applicability of this technique in diverse analytical context.[15,17,19,26-30]

Only a few reports were found exploring the SERS method for the analysis of fabrics containing noble metal nanoparticles, which are already available in several commercial products. For example, Brosseau *et al*. have studied the incorporation of Ag NPs on silk fabric, known as zari. They have developed SERS substrates to be incorporated into clothing or other textiles for the SERS monitoring of disease biomarkers and environmental pollutants.[16] Shen *et al*. have developed fabrics composed by Au NPs and cotton thread for the SERS detection of biological molecules for military and medical applications.[31] In the work presented here, we have incorporated Ag NPs on linen thread to investigate the behaviour as active SERS substrates, in particular using Raman imaging.

In this study, nanocomposites based on linen fibres and Ag NPs have been prepared through two different strategies, using *in situ* and *ex situ* methods, respectively. These composites were evaluated as SERS substrates for the detection of methylene blue (MB), used here as a model colorant for textile dyeing. We demonstrate for the first time, that the use of Raman imaging together with SERS can provide information at the level of both the nanoparticle and the molecular adsorbates distribution, with relevance in this context for monitoring textile dyeing.

2. Materials and methods

2.1. Materials

The following chemicals were used as purchased: linen fibres (commercial samples kindly supplied by CENTI, Vila Nova de Famalicão, Portugal), silver nitrate ($AgNO_3$, 99.9%, J. M. Vaz Pereira), sodium citrate tribasic dihydrate ($Na_3C_6H_5O_7 \cdot 2H_2O$, 99%, Sigma-Aldrich), methylene blue (MB, $C_{16}H_{18}N_3SCl$, Riedel-De Haën), poly(diallyldimethylammonium chloride) (PDDA, 20 wt% in water, Mw = 100,000–200,000, Aldrich) and poly(sodium 4-styrenesulfonate) (PSS, Mw = 70,000, Aldrich).

2.2. Preparation of Ag/linen nanocomposites

Ag colloids were prepared by the reduction of aqueous $AgNO_3$ using sodium citrate.[20] Briefly, an aqueous solution (50 mL) of $AgNO_3$ (1 mM) was boiled under reflux for 10 min. Then 1 mL of sodium citrate solution (1% w/v) was added dropwise to the boiling solution, under vigorous stirring. The mixture was then refluxed for 45 min and slowly cooled to room temperature.

In situ preparation of Ag/linen (**Ag/linen1**)

The *in situ* preparation of Ag/linen nanocomposites was performed using the same experimental conditions as described above for the Ag colloid preparation, by adding the linen fibres (250 mg) to the $AgNO_3$ aqueous solution previous to the reduction step. The ensuing nanocomposite fibres were then removed by filtration, thoroughly washed with deionised water and dried overnight in an oven at 70°C.

Electrostatic assembly of Ag NPs and linen fibres (**Ag/linen2**)

The *ex situ* preparation of Ag/linen nanocomposites was performed by electrostatic assembly of the components using polyelectrolytes.[10,18] Thus, aqueous solutions of PSS (1% w/v) and PDDA (1% w/v) have been prepared in NaCl aqueous solution (0.5 M). The linen textile fibres (100 mg) were surface modified using the polyelectrolytes by alternate dipping in the PDDA (20 mL), PSS (20 mL), and PDDA (20 mL) solutions. After each dipping step in the polyelectrolytes (20 min), the linen fibres were filtered and washed twice with distilled water to remove the excess of polyelectrolyte. The final step was the attachment of the Ag NPs to the linen fibres by immersing the fibres into a previously prepared Ag colloid (20 mL) for 20 min. The resulting composite was removed by filtration, washed with distilled water and dried overnight at 70°C.

2.3 SERS measurements

The **Ag/linen1** and **Ag/linen2** samples prepared as described above were investigated as SERS substrates for methylene blue (MB). Aqueous solutions of MB with varying concentrations (from 100 μM to 10 nM) have been prepared and used in order to establish the lower detection limit concentration. All samples for SERS measurements were prepared by addition of 10 μL of the MB solution to the surface of the Ag/linen nanocomposites and drying at room temperature. For all the SERS measurements the pure linen textile fibres were also used as control sample, replacing the Ag/linen nanocomposites. SERS measurements have been performed in different areas of the nanocomposites in order to check the reproducibility of the measurements.

2.4. Synthesis of dyed linen treated with Ag NPs (Ag/MB-linen)

First, 50 mg of linen fibres were stirred for 1 hour in 20 mL of an aqueous solution of MB (10^{-4}M). The fibres were then filtered, rinsed twice with distilled water and dried at room temperature. Blue coloured fibres were then stirred in an Ag colloid for different periods of time (1, 4 and 24h, respectively), and kept in the dark to avoid light degradation of MB. After stirring, the sample was filtered, rinsed twice and dried at room temperature.

2.5. Instrumentation

Inductively Coupled Plasma Atomic Emission Spectroscopy (ICP-AES), using a Jobin-Yvon JY70Plus spectrophotometer, was performed to estimate the Ag content in the final nanocomposites. A Jasco V 560 UV/Visible (UV/VIS) spectrophotometer was used for recording the UV/VIS spectra of the samples. Fourier transform infrared spectroscopy coupled to a horizontal attenuated total reflectance accessory (ATR-FTIR) was performed using a Matson 700 FTIR spectrophotometer. Scanning electron microscopy (SEM) images were obtained using a Hitachi SU-70 SEM and EDX analysis was performed using an EDX Bruker Quantax 400. Raman spectral imaging and AFM were performed in a combined Raman-AFM-SNOM confocal microscope WITec alpha300 RAS+ at CICECO, in the Chemistry Department of the University of Aveiro. A He:Ne laser operating at 633 nm was used as excitation source with the power set at 2

mW (linen based samples) and at 22 mW (MB aqueous solutions). Raman imaging experiments were performed by raster-scanning the laser beam over the samples and accumulating a full Raman spectrum at each pixel. Raman images were constructed by integrating over specific Raman bands using WITec software for data evaluation and processing. Atomic Force Microscopy in tapping mode (AC-AFM) was carried out using a tip-cantilever silicon reflex-coated with a spring constant of k = 42 N/m and 285 kHz of resonance frequency.

3. Results and discussion

Preparation and characterization of Ag/linen nanocomposites

Silver based linen fibres nanocomposites **Ag/linen1** and **Ag/linen2** were prepared by *in situ* and *ex situ* methods, respectively. In the preparation of **Ag/linen1** the silver NPs were formed *in situ* by citrate reduction of a silver salt in the presence of the linen fibres. For the preparation of **Ag/linen2** the linen fibres surface was modified with polyelectrolytes followed by addition of colloidal Ag NPs previously prepared *ex situ* by citrate reduction of a silver salt.

The linen textile fibres are composed mostly by cellulose (70%), hemicellulose (15%) and pectins (2%).[35] The cellulose moieties have a negatively charged surface in aqueous solutions over a wide range of pH due to the presence of ionizable aldehyde and carboxylate groups, that results from chemical processing.[10] Linen aqueous suspensions were found to give a zeta potential of -18.1 mV at pH 6.0, which is a value close to the value reported for vegetable cellulose fibres (-16.3 mV), due to the higher quantity of cellulose in linen fabrics.[10] Because the Ag colloid also exhibited a negative zeta potential (-25.8 mV, pH 6), the attachment of Ag NPs onto the linen textile fibres will not be a favourable event due to electrostatic repulsion. Therefore, the **Ag/linen2** nanocomposites have been obtained by attaching the Ag NPs onto linen fibres previously modified with polyelectrolytes; first with a cationic polyelectrolyte,

followed by an anionic polyelectrolyte and again with the cationic polyelectrolyte. Although this surface modification process can be subsequently repeated, it was found in our previous work[10] that a single cycle, as described above, provided cellulose fibres with homogeneous and positively charged surfaces onto which citrate coated Ag NPs strongly adhere. The Ag colloid used to prepare the **Ag/linen2** composite shows both optical and morphological features in line with the expected characteristics for Ag NPs prepared by citrate reduction.[32-34] The Ag colloid absorption spectrum presents the characteristic surface plasmon resonance (SPR) band at 446 nm, with a slight broadening due to the presence of relatively large particles (length around 100 nm; Fig. S1 in Supporting Information shows the visible absorption spectrum and a TEM image).

In the *in situ* synthesis of **Ag/linen1** the citrate reduction method in the presence of the linen fibres was used to obtain the Ag loaded nanocomposites. In this case, the reduction of cationic silver occurs presumably at the fibres surface, onto which Ag^+ ions were coordinated. Although cellulose can reduce $AgNO_3$ *in situ* due to the presence of reducing organic moieties in its surface,[5] in this research we have also used citrate as described in our previous work for the preparation of Ag/bacterial-cellulose composites that produced highly active SERS substrates.[15] Fig. 1 shows the visible absorption spectra of the Ag/linen nanocomposites and the corresponding digital photographs of the samples. The spectrum of the neat linen used as matrix is also shown for comparative purposes. The visible spectra of the nanocomposites show the characteristic SPR band of Ag NPs, at 445 nm and 418 nm for **Ag/linen1** and **Ag/linen2**, respectively.

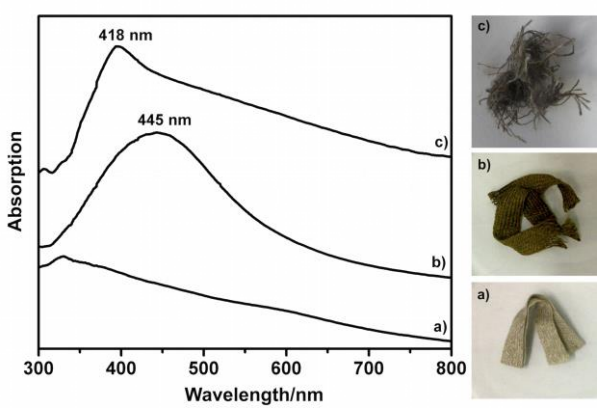

Figure 1. Visible absorption spectra (Kubelka-Munk converted reflectance spectra) and digital photographs of linen (a) and the nanocomposites **Ag/linen1** (b) and **Ag/linen2** (c).

The ATR-FTIR spectra of the Ag/linen composites prepared by the two methods are similar to the spectrum of neat linen and thereby dominated by the characteristic bands of the matrix (Fig. S2, Supporting Information). The 3200-3300 cm^{-1} region shows a large band assigned to the O-H stretching vibration. [5,36] The bands in the 2800-2980 cm^{-1} region are assigned to the C-H stretching mode and the bands at 1430 cm^{-1} and 1370 cm^{-1} are assigned to the C-H wagging (in-plane) and the C-H bending modes, respectively. The bands at 1100 cm^{-1} and 1000 cm^{-1} are assigned to the asymmetric bridge C-O-C and C-O stretching modes, respectively. The bands at 1090 and 900 cm^{-1} are assigned to the asymmetric in-plane ring stretch and asymmetric out-of-phase ring stretch, respectively.[5,36] In summary, the characteristic vibrational bands of neat linen are still observed in the final nanocomposites, thus indicating that the preparative procedures did not had a detrimental effect on the chemical identity of the textile fibres. The ATR-FTIR spectra of the Ag/linen samples are dominated by the characteristic bands of cellulose that accounts for its larger amount in these nanocomposites as compared to the other components, the polyelectrolytes included when considering **Ag/linen2** (Fig. S3, Supporting Information).

The presence of Ag NPs on the Ag/linen nanocomposites was clearly confirmed by SEM analysis, as illustrated in Fig. 2, which shows typical SEM images for the linen and the Ag/linen samples. It is clear that the smooth surfaces of the neat linen fibres turn into surfaces with higher roughness after

attachment of the Ag NPs, leading to regions enriched in Ag NPs that are distributed over the fibres surfaces. EDS analysis confirmed the presence of Ag on both nanocomposite samples. Interestingly, the SEM image of the fibres of the *in situ* sample **Ag/linen1** (Fig. 2c) also show Ag NPs in the fibres interior. This can be understood by considering that during the *in situ* synthesis the fibres might have leaked, thus exposing the interior to the subsequent attachment of the Ag NPs. Also the aqueous solution of cationic silver can also impregnate the fibres interior originating the Ag NPs inside, after reduction. In fact, the leakages observed in the **Ag/linen1** fibres might be a consequence of this growing process that, unlike in the **Ag/linen2** sample preparation, provide confined regions for Ag nucleation and growth. The amount of Ag in the fibres was evaluated by ICP giving typical values about 126 μg/g and 1230 μg/g for **Ag/linen1** and **Ag/linen2**, respectively. The difference observed for the amount of Ag in the fibres, depending on the preparative strategy, also supports the hypothesis that the growth of the Ag NPs by the *in situ* strategy might occur in confined regions defined by the fibres microstructure, which limits the Ag loading compared to the LBL method. As will be discussed later, this is an important aspect to take in consideration when producing Ag loaded textile fibres and the respective dyeing process.

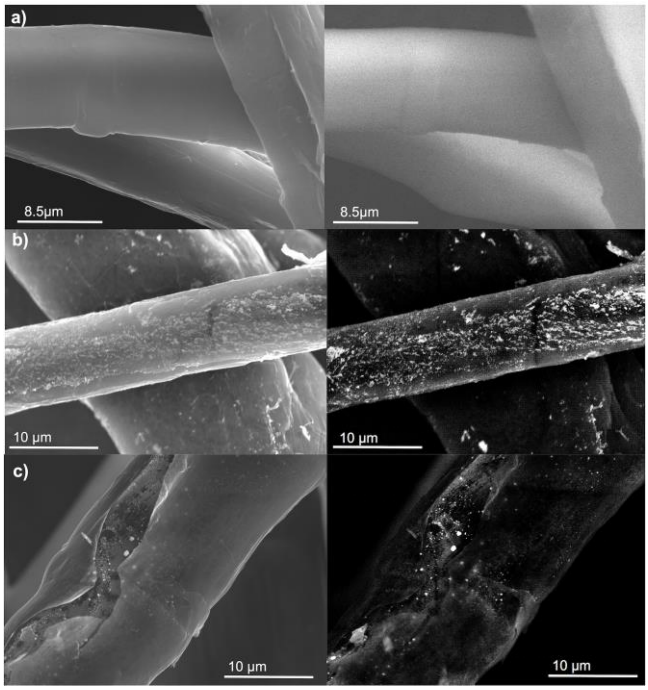

Figure 2. SEM images (left) and respective backscattered electron images (right) of a) linen textile fibres; b) **Ag/linen2** composite; c) **Ag/linen1** composite.

SERS studies using Ag/linen nanocomposites as analytical substrates

Methylene blue (MB) is a cationic heterocyclic aromatic dye that is most commonly used for colouring.[37] It belongs to the tricyclic phenothiazine family and is one of the earliest phenothiazines used as dye (structural formula in Fig. S4, Supporting Information). In the context of this work, it was found as particularly useful because it is well known to adsorb strongly to textiles such as cotton, wool and silk[38] and on the other side several Raman studies have reported a strong SERS signal when it is used as the analyte. [37,39-46]

MB aqueous solution shows absorption bands in the visible at 618 and 659 nm (Fig. 3-1). The Raman spectrum of MB aqueous solution (0.1 M), using the 633 nm excitation line, is presented in Fig. 3-2. The strong absorption of MB at 633 nm can induce a resonance Raman effect when this laser line is used. The Raman spectra of the linen textile fibres and Ag/linen composites are presented in Fig. S5 (see Supporting Information).

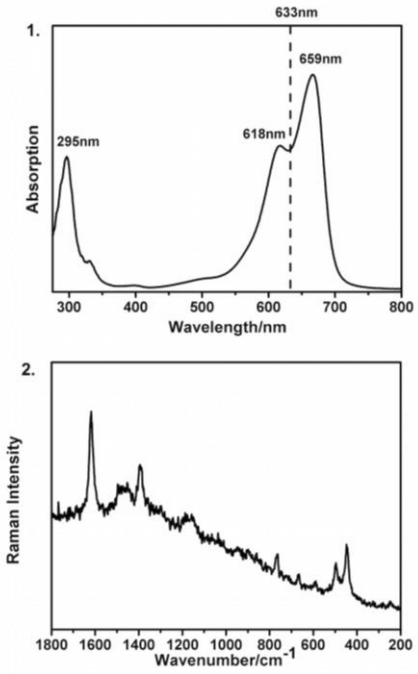

Figure 3. (1) Optical spectrum of MB. (2) Conventional Raman spectrum of MB aqueous solution (0.1 M) (excitation at 633 nm, 22 mW laser power, 10 scans with 0.5 s acquisition time each).

Figure 4-b,c show the SERS spectra of MB after placing aliquots of a 10^{-4} M solution onto the Ag/linen samples. The Ag/linen nanocomposites act as SERS substrates due to the presence of the Ag NPs. Indeed, the linen textile fibres without Ag NPs were also used instead of the composites and the Raman signal for MB was not observed (Fig. 4-a). The SERS signal corresponding to the diagnosis band at 1620 cm^{-1} was still observed for MB aqueous solutions with concentration as low as 10^{-8} M, when using the **Ag/linen2** composite as substrate (Fig. S6, see Supporting Information). Fig. 4 also shows that in these conditions there are no significant differences in the SERS spectra of MB using as substrates either composites **Ag/linen1** or **Ag/linen2**. However some differences arise when comparing to the conventional Raman of a MB aqueous solution (Fig.3-2). In particular, the band at 475 cm^{-1}, which has been assigned to the ν(CN)+ν(CC) and thiazine in-plane bending modes[47] (Table 1), is strongly enhanced in the SERS spectrum of MB, suggesting preferential chemisorption of MB on the Ag surface through the ring nitrogen and in a perpendicular or tilted position to the surface.[48] There are also additional Raman bands in the SERS spectra, such as those at 1035 and 887 cm^{-1}, which might equally result from a chemical effect enhancement.[26,42] Table 1 lists the Raman shifts and respective assignments observed in the Raman spectra of MB aqueous solutions collected with a 633 nm laser, using conventional conditions and in the SERS substrates **Ag/linen1** and **Ag/linen2**.

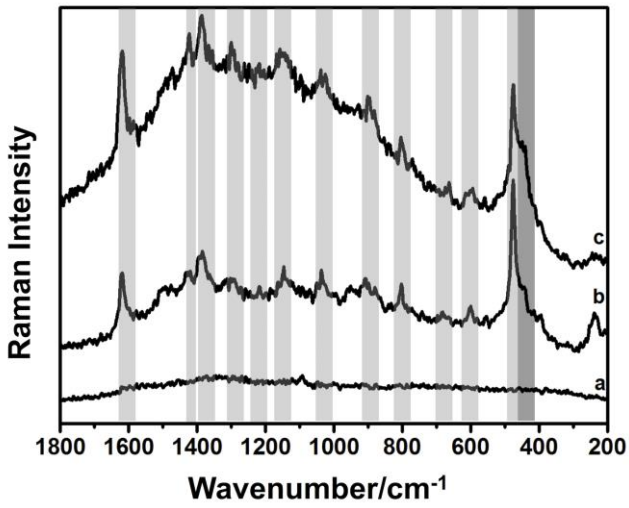

Figure 4. a) Raman spectrum of linen with a drop of MB (10^{-4}M); SERS spectra of MB (10^{-4}M) using b) **Ag/linen2** and c) **Ag/linen1** composites as substrates (excitation at 633 nm, 2 mW laser power, 10 scans with 0.5 s acquisition time each).

In order to explore the possibility of Raman imaging of MB dye over the Ag loaded linen fibres, the spatial distribution of the MB on the Ag/linen composites surface was evaluated for the best SERS recording conditions. Fig. 5 shows the optical micrographs together with the respective 2D Raman images of MB, using the Ag/linen nanocomposites as SERS substrates. Raman imaging was performed by raster-scanning the laser beam over a surface area around 45 x 60 μm and accumulating a full Raman spectrum at each pixel. Raman images were constructed by integrating over the MB band at 1620 cm^{-1}. Thus, stronger SERS signal intensities from MB indicate higher amounts of the molecular probe shown by a brighter colour in Fig.5. It also indicates the position of the Ag particles in the fibre considering that the SERS signal can only be obtained for MB adsorbed on the Ag surface. The Raman imaging of the MB using **Ag/linen2** as SERS substrate (Fig. 5-a) shows that the MB molecules and the respective Ag particles (where the MB molecules adsorbed) are well dispersed along the textile fibres, which agrees with the SEM images previously shown in Fig. 2-b where the Ag NPs also show identical distribution over the linen fibres. On the other hand, the Raman imaging of MB using **Ag/linen1** as SERS substrate (Fig. 5-b) shows regions of higher intensity in specific areas of the fibres, which can be due to the presence of Ag NPs agglomerates, a result that is also in agreement with the SEM analysis (Fig. 2-c).

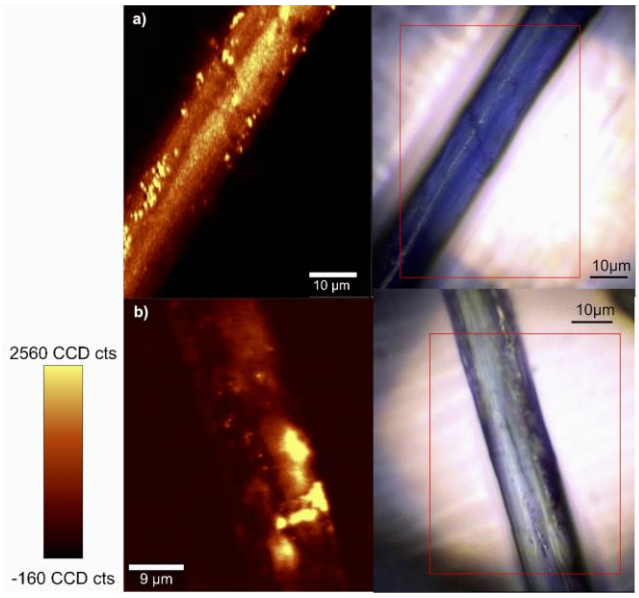

Figure 5. Raman images obtained using the integrated intensity of the Raman band at 1620 cm^{-1} in the SERS spectra of MB 10^{-4}M using the composites (a) **Ag/linen2** and (b) **Ag/linen1** as substrates (excitation at 633 nm, 2 mW laser power, 150 points per line x 150 lines per image,

0.02s). The respective optical images of the samples are on the right side, with the scanned area marked in red. The vertical bar shows the colour profile in a) and b) images, with the relative intensity scale.

The results above show the importance of SERS imaging to probe the surface distribution of Ag NPs in antimicrobial textile fibres, in this particular case using MB as analyte. MB is also a good example of an organic dye for textiles that can be followed by SERS in the presence of Ag NPs. Following this approach, we decided to inquire the possibility to probe the presence of Ag NPs in the interior of the fibres. Hence, Raman imaging experiments have been conducted by monitoring the SERS signal of MB (band at 1620 cm^{-1}) along the z-axis. Fig. 6 shows the optical micrographs together with 2D in-depth Raman imaging for the Ag/linen textile fibres prepared by the *ex situ* and *in situ* methods. The Raman images were collected by raster-scanning the laser beam over a surface area with 10 μm in depth, by accumulating a full Raman spectrum at each pixel. In-depth Raman imaging of MB using the **Ag/linen2** sample shows intense SERS signal predominantly at the surface of the linen fibres. This observation confirms the distribution of Ag NPs on the nanocomposite surface, forming a nanostructured coating wrapping the linen fibres and making a thin film. On the other hand, in the in-depth Raman imaging using the **Ag/linen1** as SERS substrate, it is still possible to detect a Raman signal of MB also when focusing the laser inside the fibres. This observation is in line with the hypothesis presented before that assumes that for the *in situ* preparation of **Ag/linen1**, probably there is diffusion of cationic silver into the fibres interior, allowing nucleation and growth of Ag NPs that ultimately can create leaks in the fibres.

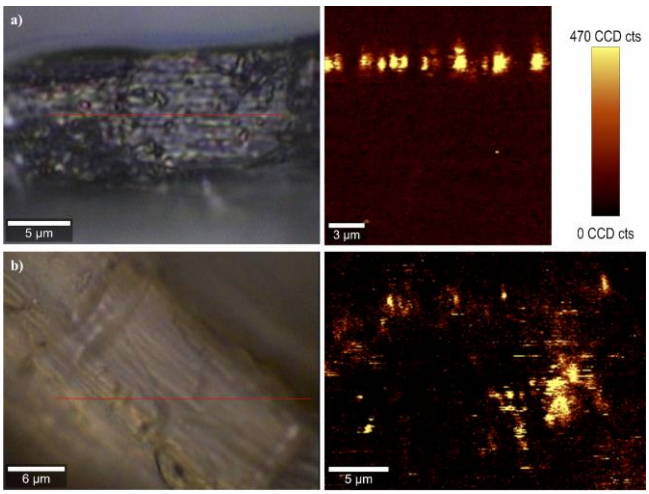

Figure 6. Optical images of (a) **Ag/linen2** and (b) **Ag/linen1** marked with a red line that indicates the beginning of the respective in-depth Raman image shown on the right side. The Raman images were obtained using the integrated intensity of the band at 1620 cm^{-1} in the SERS spectra of MB 10^{-4} M in the Ag/linen substrates (excitation at 633nm, 2 mW laser power, 150 points per line x 150 lines per image, 0.02s). The vertical bar shows the colour profile in the Raman images, with the relative intensity scale.

Additional evidence for the distinct types of distribution of Ag NPs on the linen textile fibres surface, depending on the preparative method employed, was provided by AFM analysis (Fig. 7). For the **Ag/linen2** composite the AFM topography images show Ag NPs distributed uniformly over the surface, while for the **Ag/linen1** composite smaller and more dense regions in Ag NPs have been observed. A cross section was also recorded to verify the size of the Ag NPs (see Fig. S7 in Supporting Information) and the size distribution is around 100 nm and 70 nm for **Ag/linen2** and **Ag/linen1**, respectively.

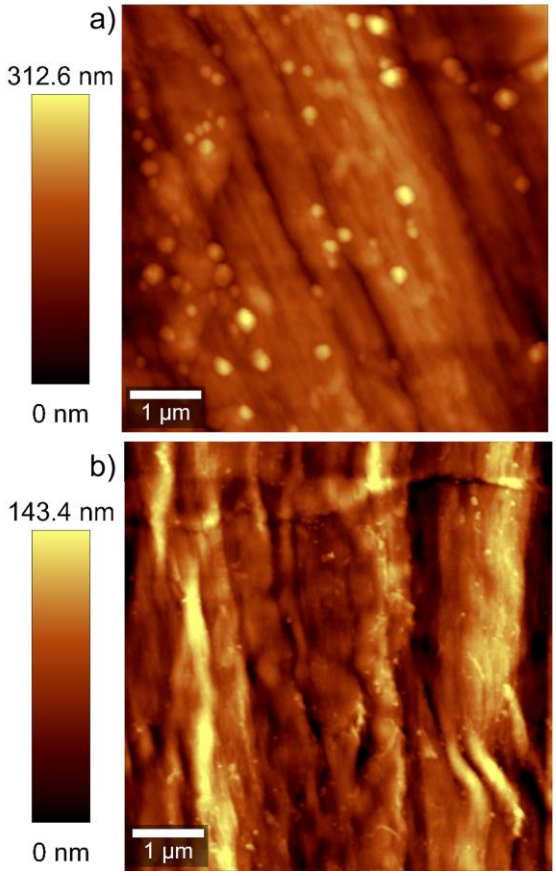

Figure 7. AFM topography images (6 µm x 6 µm) of Ag/linen nanocomposites: a) **Ag/linen2** and b**) Ag/linen1**. The vertical bars show the colour profile in a) and b) images, respectively, with the relative intensity scales.

Considering all the experimental data shown above, there is clear evidence that Raman imaging and in particular SERS imaging can be used to monitor the distribution of Ag NPs in linen fibres in the presence of MB. However, the results presented so far were obtained for linen fibres previously loaded with Ag NPs and then treated with MB solution. It is also of great interest to study this process on previously dyed fibres that have subsequently been put in contact with Ag NPs (*eg.* an Ag colloid). In this experiment, an aqueous solution of MB (10^{-4}M) was first vigorously stirred for 1 hour in the presence of linen fibres. Due to its positive charge in aqueous solution at pH 6, the MB molecules are electrostatically attracted to the negatively charged linen surfaces. The obtained coloured MB-linen fibres were then exposed to a citrate coated Ag colloid (negatively charged) for increasing contact times and chemisorption between silver surfaces and MB molecules is expected to occur. Fig. 8 shows the Raman images collected by raster-scanning the laser beam over a surface area with 45 x 60 μm and accumulating a full Raman spectrum at each pixel, and constructed by integrating over the MB band at 1620 cm^{-1}. The Raman image of MB-linen fibres in the absence of Ag NPs was also recorded and did not show bright regions at the same scale of intensity used for the other Raman images (Fig. 8). Also note that in this case the spectrum of the dyed fibres showed significant fluorescence contribution from the adsorbed MB molecules (Figure S8). As the contact time of the MB-linen fibres with the Ag colloid was increased, the corresponding mapping images revealed more brighter regions which is ascribed to the enhancement of the Raman signal of MB at 1620 cm^{-1}. Indeed, inspection of the Raman spectra (Figure S8) of the dyed linen samples when treated with Ag NPs, shows that the Raman band at 1620 cm^{-1} became more pronounced as the contact time with the silver colloid was increased. After 24 hours contact time, the Raman imaging results indicates that the Ag NPs end up distributed all over the linen fibers surfaces.

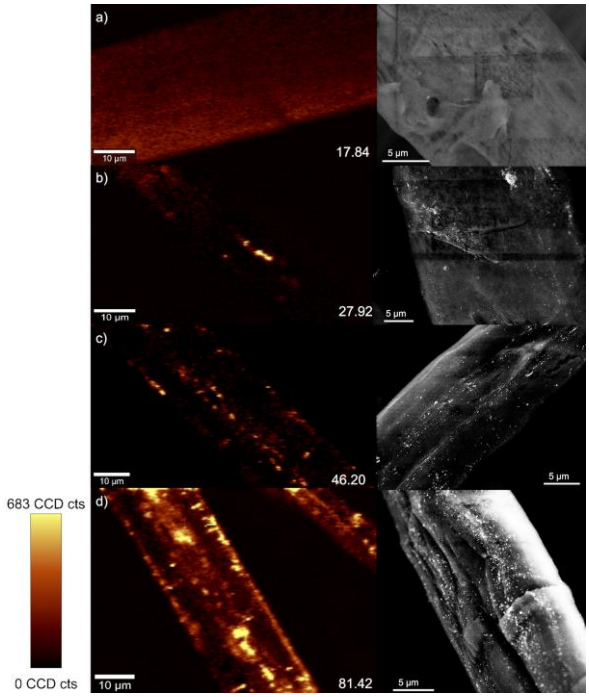

Figure 8. Raman images obtained (using the integrated intensity of the MB band at 1620 cm^{-1}) from the Raman spectra of a) MB dyed fibres; and from the SERS spectra of composites made of MB dyed fibres added to Ag colloids for b) 1h; c) 4h; d) 24h (excitation at 633 nm, 2mW laser power, 150 points per line x 150 lines per image, 0.02s). The vertical bar shows the colour profile and the relative intensity scale. Inset: Values of average intensity of the band at 1620 cm^{-1}. Backscattered SEM images of the respective samples are shown on the right side.

Conclusions

The ability of applying Raman imaging techniques together with SERS for the characterization of textile fibres loaded with Ag NPs was here firstly demonstrated. The relevance of this approach towards functional fabrics characterization arises also by the fact that non-destructive Raman techniques are employed. Although the study was here focused on linen fibres dyed with methylene blue, in principle it is possible to extend this strategy to other types of textiles and dyes. A better understanding of how Ag NPs are incorporated in textile fibres, namely in finished fabrics, is of current interest due to the widespread of these nanocomposites in antimicrobial products. Although other techniques are available for such purposes, this research has shown that Raman imaging and SERS are valuable assets that complement or eventually provide unique characterization data.

Acknowledgements

This work was developed within the scope of the project CICECO-Aveiro Institute of Materials, POCI-01-0145-FEDER-007679 (FCT Ref. UID /CTM /50011/2013), financed by national funds through the FCT/MEC and when appropriate co-financed by FEDER under the PT2020 Partnership Agreement. S. Fateixa thanks Fundação para a Ciência e Tecnologia (FCT) for the Grant SFRH/BPD/93547/2013.

References

[1] K. Qi, J. H. Xin, *ACS Appl. Mater. Interfaces*, **2010**; *2*, 3479.

[2] Q. Wei, L. Yu, D. Hou, F. Huang, *J. Appl. Polym. Sci*. **2008**; *107*, 132.

[3] Y. Cai, F. Huang, Q. Wei, E. Wu, W. Gao, *Appl. Surf. Sci.* **2008**; *254*, 5501.

[4] A. R. Horrocks, S. Nazaré, R. Masood, B. Kandola, D. Price, *Polym. Adv. Technol.* **2011**; *22*, 22.

[5] M. Montazer, F. Alimohammadi, A. Shamei, M. K. Rahimi, *Carbohydr. Polym.* **2012**; *87*, 1706.

[6] F. Alimohammadi, M. P. Gashti, A. Shamei, *Prog. Org. Coatings*, **2012**; *74*, 470.

[7] M. P. Gashti, F. Alimohammadi, A. Shamei, *Surf. Coatings Technol*. **2012**; *206*, 3208.

[8] R. Dastjerdi, M. Montazer, *Colloids Surfaces B Biointerfaces*, **2010**; *79*, 5.

[9] R. J. B. Pinto, M. C. Neves, C. P. Neto, T. Trindade, *in Nanocomposites - New Trends and Developments*, (Ed: Dr. Farzad Ebrahomi) **2012**, pp. 73–96.

[10] N. C. T. Martins, C. S. R. Freire, R. J. B. Pinto, S. C. M. Fernandes, C. P. Neto, A. J. D. Silvestre, J. Causio, G. Baldi, P. Sadocco, T. Trindade, *Cellulose*, **2012**; *19*, 1425.

[11] S. T. Dubas, P. Kumlangdudsana, P. Potiyaraj, *Colloids Surfaces A Physicochem. Eng. Asp*. **2006**; *289*, 105.

[12] J. Scholz, G. Nocke, F. Hollstein, A. Weissbach, *Surf. Coatings Technol.* **2005**; *192*, 252.

[13] N. G. Bastús, F. Merkoçi, J. Piella, V. Puntes, *Chem. Mater*. **2014**; *26*, 2836.

[14] L. Pourzahedi M. J. Eckelman, *Environ. Sci. Technol*. **2015**; *49*, 361.

[15] P. A. A. P. Marques, H. I. S. Nogueira, R. J. B. Pinto, C. P. Neto, T. Trindade, *J. Raman Spectrosc.* **2008**; *39*, 439.

[16] A. M. Robinson, L. Zhao, M. Y. Shah Alam, P. Bhandari, S. G. Harroun, D. Dendukuri, J. Blackburn, C. L. Brosseau, *Analyst* **2015**; *140*, 779.

[17] S. Abalde-Cela, S. Ho, B. Rodríguez-González, M. A. Correa-Duarte, R. A. Álvarez-Puebla, L. M. Liz-Marzán, N. A. Kotov, *Angew. Chemie Int. Ed*. **2009**; *48*, 5326.

[18] R. J. B. Pinto, P. A. Marques, M. A. Martins, C. P. Neto, T. Trindade, *J. Colloid Interface Sci.* **2007**; *312*, 506.

[19] M. Rycenga, C. M. Cobley, J. Zeng, W. Li, C. H. Moran, Q. Zhang, D. Qin, Y. Xia, *Chem. Rev.* **2011**; *111*, 3669.

[20] P. C. Lee, D. Meisel, *J. Phys. Chem.* **1982**; *86*, 3391.

[21] K. A. Willets, R. P. Van Duyne, *Annu. Rev. Phys. Chem.* **2007**; *58*, 267.

[22] J. Kneipp, H. Kneipp, K. Kneipp, *Chem. Soc. Rev.* **2008**; *37*, 1052.

[23] H. Xu, E. J. Bjerneld, M. Ka¨ll, L. Börjesson, *Phys. Rev. Lett.* **1999**; *83*, 4357.

[24] E. Hao, G. C. Schatz, *J. Chem. Phys.* **2004**; *120*, 357.

[25] A. M. Michaels, M. Nirmal, L. E. Brus, *J. Am. Chem. Soc.* **1999**; *121*, 9932.

[26] G. N. Xiao, S. Q. Man, *Chem. Phys. Lett.* **2007**; *447*, 305.

[27] A. Bonifacio, S. Cervo, V. Sergo, *Anal. Bioanal. Chem.* **2015**; *407*, 8265.

[28] A. Hakonen, P. O. Andersson, M. Stenbæk Schmidt, T. Rindzevicius, M. Käll, *Anal. Chim. Acta* **2015**; *893*, 1.

[29] H. Wei, S. M. Hossein Abtahi, P. J. Vikesland, *Environ. Sci. Nano* **2015**; *2*, 120.

[30] S. Fateixa, H. I. S. Nogueira, T. Trindade, *Phys. Chem. Chem. Phys.* **2015**; *17*, 21046.

[31] D. R. Ballerini, Y. H. Ngo, G. Garnier, B. P. Ladewig, W. Shen, P. Jarujamrus, *AIChE J*. **2014**; *60*, 1598.

[32] S. Fateixa, S. F. Soares, A. L. Daniel-da-Silva, H. I. S. Nogueira, T. Trindade, *Analyst* **2015**; *140*, 1693.

[33] J. P. Camden, J. A. Dieringer, Y. Wang, D. J. Masiello, L. D. Marks, G. C. Schatz, R. P. Van Duyne, *J. Am. Chem. Soc.* **2008**; *130*, 12616.

[34] Z. S. Pillai, P. V. Kamat, *J. Phys. Chem. B* **2004**; *108*, 945.

[35] M. J. John, R. D. Anandjiwala, *Polymer Composites* **2008**; *29*. 187.

[36] C. Chung, M. Lee, E. K. Choe, *Carbohydr. Polym*. **2004**; *58*, 417.

[37] N. G. Tognalli, A. Fainstein, C. Vericat, M. E. Vela, R. C. Salvarezza, *J. Phys. Chem. B* **2006**; *110*, 354.

[38] B. A. Fil, C. Ozmetin, M. Korkmaz, *Bull. Korean Chem. Soc.* **2012**; *33*, 3184.

[39] S. H. A. Nicolai, J. C. Rubim, *Langmuir* **2003**, *19*, 4291.

[40] P. H. B. Aoki, P. Alessio, A. Riul, Jr., J. A. de Saja Saez, C. J. L. Constantino, *Anal. Chem.* **2010**, *82*, 3537.

[41] S.-H. Seo, B.-M. Kim, A. Joe, H.-W. Han, X. Chen, Z. Cheng, E.-S. Jang, *Biomaterials* **2014**, *35*, 3309.

[42] X. Dong, H. Gu, J. Kang, X. Yuan, J. Wu, *Colloids Surfaces A Physicochem. Eng. Asp*. **2010**, *368*, 142.

[43] Z. Gan, A. Zhao, M. Zhang, W. Tao, H. Guo, Q. Gao, R. Mao, E. Liu, *Dalton Trans.* **2013**; *42*, 8597.

[44] P. H. B. Aoki, P. Alessio, J. A. de Saja, C. J. L. Constantino, *J. Raman Spectrosc.* **2010**; *41*, 40.

[45] S. H. Toma, J. J. Santos, K. Araki, H. E. Toma, *Anal. Chim. Acta* **2015**; *855*, 70.

[46] D.-S. Tira, M. Potara, S. Astilean, *Mater. Res. Bull.* **2015**; *64*, 267.

[47] P. H. B. Aoki, D. Volpati, W. Caetano, and C. J. L. Constantino, *Vib. Spectrosc.* **2010**; *54*, 93.

[48] H. I. S. Nogueira, Spectrochimica Acta A **1998**; *54*, 1461.

[49] L. Zhong, Y. Hu, D. Xing, *in Pacific Rim Conference on Lasers and Electro-Optics*, CLEO - Technical Digest, **2009**, n/n.

[50] S. Sarkar, S. Pande, S. Jana, A. K. Sinha, M. Pradhan, M. Basu, J. Chowdhury, T. Pal, *J. Phys. Chem. C* **2008**; *112*, 17862.

Table1: Conventional Raman data for Methylene Blue (10^{-1} M concentration) and SERS of MB (10^{-4}M) using Ag/line nanocomposites at distinct excitation laser sources (wavenumbers in cm^{-1}, relative intensity[a]).

Raman MB (10^{-1} M) *in Fig. 3-2*	SERS MB (10^{-4} M) using Ag/linen2 *in Fig. 4b*	SERS MB (10^{-4} M) using Ag/linen1 *in Fig. 4c*	Assignments[b; 26,42,47,49,50]
1618 vs	1622 s	1618 vs	ν (CC) + δ (CH) in plane (ring), ν (CN) + ν (CC)
1485 w	1484 vw	1484 w	ν_{sym} (CN) (lateral) + δ (CH) in plane (ring) + δ (CH) out of plane (CH_3), ν (CC)
1430 w	1426 vw	1425 w	δ (CH) out of plane (CH_3), ν (CC), ν_{sym} (CN)
1392 m	1392 m	1392 m	ν_{sym} (CN) (lateral and center) + δ (CH) in plane (ring) + δ (CH) out of plane (CH_3), ν (CN) + ν (CC), ν_{asym} (CN)
------	1298 vw	1299 w	ν_{sym} (CN) (center) + δ (CH) in plane (ring), ν (CC)
1181 w	1147 w	1156 w	δ (CH) in plane (ring) + δ (CH) out of plane (CH_3), δ (CH) in plane
-----	1035 w	1039 w	ν_{asym} (CS) + δ (CH) in plane (ring) + δ (CH) out of plane (CH_3), ν_{asym} (CS), δ (CH) in plane
-----	887 w	872 w	Skeletal deformation (CC), δ (CH) in plane
770 m	770 w	770 w	Skeletal deformation (CN and CH_3), δ (CH) in plane
677 w	681 vw	667 vw	Skeletal deformation (CC), δ (CH) in plane
583 vw	603 vw	603 vw	Torsion of molecule + δ (CH) out of plane (ring), CC skeletal deformation
496 m	481 vs	475 vs	Thiazine ring in-plane bending
441 s	446 m	441 m	Skeletal deformation (CN, CS and CH_3), CN skeletal deformation

[a] Relative intensities: vs – very strong; s – strong; m – medium; w – weak; vw – very weak; [b] δ - bending, ν – stretching.